ESC European Society of Cardiology

Europace (2023) **25**, 739–747
https://doi.org/10.1093/europace/euac187

BASIC SCIENCE

Quantitative assessment of transmural fibrosis profile in the human atrium: evidence for a three-dimensional arrhythmic substrate by slice-to-slice histology

Flavia Ravelli [1,2]*, Michela Masè[1]†, Alessandro Cristoforetti [1], Laura Avogaro[1], Elvira D'Amato[3], Francesco Tessarolo [4], Federico Piccoli[5], and Angelo Graffigna[6]

[1]Laboratory of Biophysics and Translational Cardiology, Department of Cellular, Computational and Integrative Biology—CIBIO, University of Trento, 38123 Trento, Italy; [2]CISMed—Centre for Medical Sciences, University of Trento, Trento, Italy; [3]Department of Physics, University of Trento, Trento, Italy; [4]Department of Industrial Engineering and BIOtech, University of Trento, Trento, Italy; [5]Department of Laboratory Medicine, Santa Chiara Hospital, Trento, Italy; and [6]Department of Cardiac Surgery, Santa Chiara Hospital, Trento, Italy

Received 29 April 2022; accepted after revision 30 September 2022; online publish-ahead-of-print 9 November 2022

Aims

Intramural fibrosis represents a crucial factor in the formation of a three-dimensional (3D) substrate for atrial fibrillation (AF). However, the transmural distribution of fibrosis and its relationship with atrial overload remain largely unknown. The aim of this study is to quantify the transmural profile of atrial fibrosis in patients with different degrees of atrial dilatation and arrhythmic profiles by a high-resolution 3D histology method.

Methods and results

Serial microtome-cut tissue slices, sampling the entire atrial wall thickness at 5 μm spatial resolution, were obtained from right atrial appendage specimens in 23 cardiac surgery patients. Atrial slices were picrosirius red stained, imaged by polarized light microscopy, and analysed by a custom-made segmentation algorithm. In all patients, the intramural fibrosis content displayed a progressive decrease alongside tissue depth, passing from 68.6 ± 11.6% in the subepicardium to 10–13% in the subendocardium. Distinct transmural fibrotic profiles were observed in patients with atrial dilatation with respect to control patients, where the first showed a slower decrease of fibrosis along tissue depth (exponential decay constant: 171.2 ± 54.5 vs. 80.9 ± 24.4 μm, $P < 0.005$). Similar slow fibrotic profiles were observed in patients with AF (142.8 ± 41.7 μm). Subepicardial and midwall levels of fibrosis correlated with the degree of atrial dilatation ($\rho = 0.72$, $P < 0.001$), while no correlation was found in subendocardial layers.

Conclusions

Quantification of fibrosis transmural profile at high resolution is feasible by slice-to-slice histology. Deeper penetration of fibrosis in subepicardial and midwall layers in dilated atria may concur to the formation of a 3D arrhythmic substrate.

* Corresponding author. Tel: +39 0461 882776. *E-mail address*: flavia.ravelli@unitn.it
† Present address: Institute of Mountain Emergency Medicine, EURAC Research, Bolzano, Italy.

Graphical Abstract

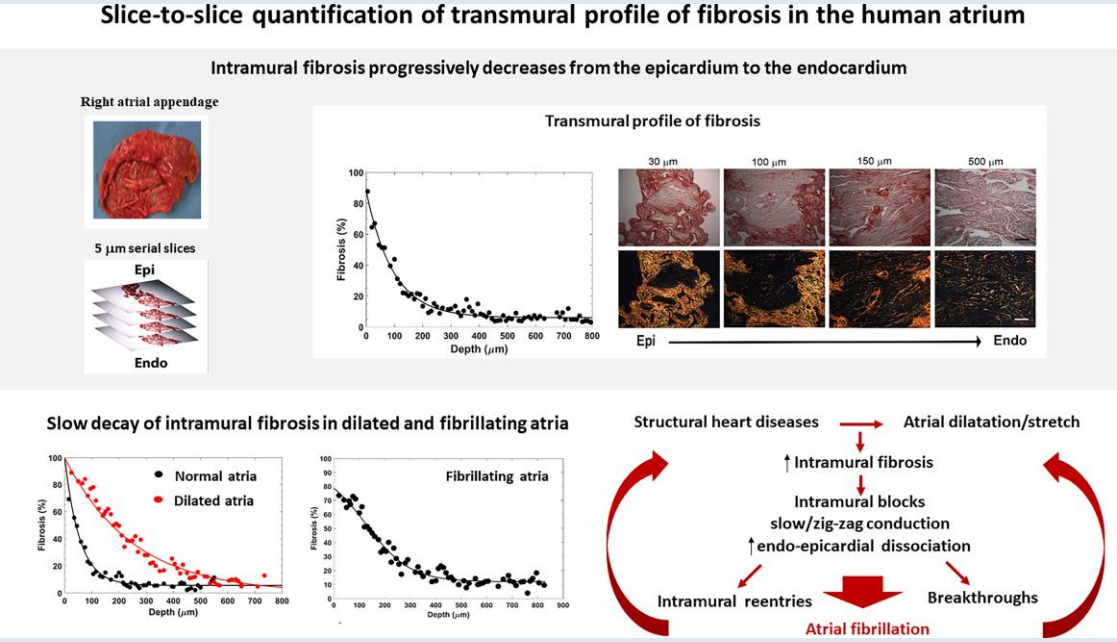

Keywords Fibrosis • Atrial fibrillation • Atrial overload • Structural remodelling • Myocardial slices

What's new?

- Quantification of fibrosis transmural profile at high spatial resolution is feasible in human atrial tissue by slice-to-slice histology and may be useful for evaluating the three-dimensional (3D) substrate of atrial fibrillation (AF).
- Fibrosis profile displays a progressive decrease alongside tissue depth, from the epicardium to the endocardium in all patients.
- A fast epi-endocardial decay was observed in patients with normal atrial size.
- Patients with atrial dilatation and patients with AF show a slower decay with higher penetration of fibrosis in the subepicardial and midwall layers, which may contribute to the formation of a 3D arrhythmic substrate.

Introduction

Fibrosis represents a pathological condition, characterized by fibroblast proliferation, differentiation into myofibroblasts, and increased production of extracellular matrix components, with predominance of collagen. The fibrotic cellular response is regulated by a complex net of signalling pathways and can be promoted by a variety of noxious stimuli, including mechanical stretch.[1,2] Accumulating evidence indicates myocardial fibrosis as a fundamental player in the structural remodelling that supports the initiation and maintenance of ventricular tachyarrhythmias[3] and atrial fibrillation (AF).[1] Fibrosis may contribute to AF through several mechanisms, creating a vulnerable substrate for re-entrant activity and promoting the emergence of triggers.[4–6]

Although the degree of structural remodelling and the global amount of fibrosis are crucial factors for the stability of AF, it has become evident that the spatial distribution and type of fibrosis may be at least as important.[4–8] In particular, the presence of fibrosis between the thin epicardial layer and the endocardial bundle network may exacerbate endo-epicardial dissociation. This may transform the atrial wall into a complex and heterogeneous three-dimensional (3D) medium for wavelet propagation, characterized by delayed and out-of-phase layer activation and increased occurrence of breakthroughs.[9,10]

Despite the importance of the spatial distribution of fibrosis as a key determinant of AF, few studies, mainly based on indirect imaging techniques with low spatial resolution, reported human data on intramural fibrosis distribution.[5,7,8] Conversely, gold standard histological assessment of human atrial samples in previous studies was limited to a global evaluation of fibrosis amount.[11,12]

To fill this gap, the present study aimed at: (i) reconstructing the pattern of transmural fibrosis from human atrial tissue samples and (ii) assessing the relationship between intramural fibrosis, chronic atrial stretch, and arrhythmic profiles. High-resolution fibrosis transmural profiles were reconstructed by a computerized 3D histology approach applied to serial microtome-cut longitudinal slices covering the whole atrial wall. Fibrosis patterns were then compared in patients characterized by distinct atrial dilatation grades and arrhythmic profiles.

Methods

Patient population and human tissue collection

Tissue samples were excised from the right atrial appendage in 23 patients (four females, mean age 68.9 ± 9.8 years) undergoing aortic or mitral valve replacement with extracorporeal circulation at the Santa Chiara Hospital of Trento. Eight patients had documented long-standing persistent AF (duration ≥1 year), while the remaining patients presented no history of AF. Basic demographic and clinical information, including sex, age, and associated comorbidities,

Table 1 Demographic and clinical description of the overall patient population and the three analysed subgroups

Patient characteristics	Overall population	Ctrl group	AD group	AF group	*P*-values
Number of patients	23	8	7	8	
Age (years)	68.9 ± 9.8	66.1 ± 12.3	68.4 ± 9.8	72.3 ± 6.9	0.47
Men, *n* (%)	19 (82.6)	7 (87.5)	6 (85.7)	6 (75)	0.78
Female, *n* (%)	4 (17.4)	1 (12.5)	0 (0)	1 (12.5)	0.62
LA enlargement grade	2 (0.25–3)	0 (0–0.5)	2 (2–3)	3 (1.5–3)	<0.001
LVEF, %	60 (58–67.7)	63.8 ± 5.4	61.7 ± 11.8	55.9 ± 13.7	0.34
Comorbidities					
Aortic valve disease, *n* (%)	17 (73.9)	7 (87.5)	5 (71.4)	5 (62.5)	0.51
Mitral valve disease, *n* (%)	7 (30.4)	1 (12.5)	1 (14.3)	5 (62.5)	0.051
Coronary artery disease, *n* (%)	2 (8.7)	1 (12.5)	0 (0)	1 (12.5)	0.62
Ischemic cardiomyopathy, *n* (%)	3 (13.0)	2 (25)	0 (0)	1 (12.5)	0.36
Angina pectoris, *n* (%)	6 (26.1)	2 (25)	3 (42.9)	1 (12.5)	0.41
COPD, *n* (%)	3 (13.0)	1 (12.5)	0 (0)	2 (25)	0.36
Diabetes mellitus, *n* (%)	5 (21.7)	1 (12.5)	2 (28.6)	2 (25)	0.72
Hypertension, *n* (%)	15 (65.2)	4 (50)	4 (57.1)	7 (87.5)	0.25
Renal insufficiency, *n* (%)	1 (4.3)	0 (0)	0 (0)	1 (12.5)	0.38
Metabolic disease, *n* (%)	4 (17.4)	2 (25)	0 (0)	2 (25)	0.35
Heart failure, *n* (%)	4 (17.4)	1 (12.5)	1 (14.3)	2 (25)	0.78
Intervention					
Isolated AVR, *n* (%)	11 (47.8)	5 (62.5)	4 (57.1)	2 (25)	0.27
Isolated MVR, *n* (%)	2 (8.7)	1 (12.5)	0 (0)	1 (12.5)	0.62
Combined AVR and CABG, *n* (%)	5 (21.7)	2 (25)	2 (28.6)	1 (12.5)	0.72
Combined MVR and CABG, *n* (%)	3 (13.0)	0 (0)	1 (14.3)	2 (25)	0.33
Combined AVR and CABG, *n* (%)	2 (8.7)	0 (0)	0 (0)	2 (25)	0.13

The three patient groups correspond to control patients (Ctrl), patients with atrial dilatation (AD), and patients with atrial fibrillation (AF). Data are numbers (*n*) and percentages (%), mean ± standard deviation or median (interquartile range), as pertinent. Statistical differences among subgroups were consistently assessed by Pearson's χ^2, ANOVA, or Kruskal–Wallis tests.
AVR, aortic valve replacement; CABG, coronary artery bypass grafting; LA, left atrium; LVEF, left-ventricular ejection fraction; MVR, mitral valve replacement.

was acquired in all patients and is reported in *Table 1*. Preoperative two-dimensional transthoracic echocardiography was routinely performed in each patient. Atrial size (atrial linear dimensions, atrial area, and/or atrial volume) was measured (see Supplementary material online, *Table S1*) and the level of left atrial enlargement was graded as: Grade 0 = reference range/normal, Grade 1 = mildly abnormal, Grade 2 = moderately abnormal, Grade 3 = severely abnormal, according to the criteria in Lang *et al.*[13] (see Supplementary material online, *Table S2*). The investigation was approved by the Ethical Committee for Clinical Experimentation of the Provincial Agency for Health Services of the Autonomous Province of Trento and conformed to the principles outlined in the declaration of Helsinki. All patients gave written informed consent.

Tissue slice preparation

A detailed description of tissue sample collection and preparation is provided in the Supplementary material online. Briefly, specimens of few mm^2 surface dimension, encompassing the entire atrial wall thickness, were excised, pre-processed, and embedded in paraffine. Epicardial and endocardial surfaces were identified, and samples were cut into serial longitudinal sections (i.e. slices cut tangentially to the epicardial/endocardial layer) of 5 μm thickness by a rotary microtome (Leica RM2245; Leica Biosystems, Milan, Italy; *Figure 1A*). After pre-treatment, tissue sections were stained with 0.1% solution of Sirius Red F3BA (Direct Red 80, CI 35780; Sigma Aldrich, Milan, Italy) in saturated aqueous solution of picric acid, rinsed in acidified water and 70% ethanol, dehydrated, and finally mounted with a drop of mounting medium and a glass cover slip.

Imaging and quantification of fibrosis

A total of 1209 picrosirius red–stained sections were examined by light microscopy (DMIL microscope combined with DFC420 camera; Leica, Germany) and acquired both in bright field and polarized light. Collagen detection was based on the birefringence effect of the sample under polarized light. Captured images were analysed using a custom-made Matlab software, which analysed both the bright-field and dark-field images to detect the tissue area and the collagen area, respectively (*Figure 1B*). The analysis workflow included a pre-processing step, which was meant to address limitations in the acquisition set-up, and a detection step, which was based on a semi-automatic, human-supervised threshold-based segmentation approach, similar to previous studies.[14] The collagen fraction was computed as the percentage of the collagen area over the total segmented tissue area. A detailed description of the methodology for fibrosis quantification is provided in the Supplementary material online.

The 3D collagen profile was obtained in each patient by displaying the fraction of collagen in subsequent tissue slices as a function of slice distance from the epicardial surface. Exponential or sigmoidal functions were fit to the paired data by nonlinear least square method and the spatial decay constant of the process was estimated. The goodness of fit was assessed by adjusted *r*-squared and root mean squared error (rmse). In each patient, fibrosis content was quantified separately for the outer/subepicardial (0–30% distance ratio from the epicardial surface), midwall (30–60% distance ratio), and inner/subendocardial layers (60–100% distance ratio).

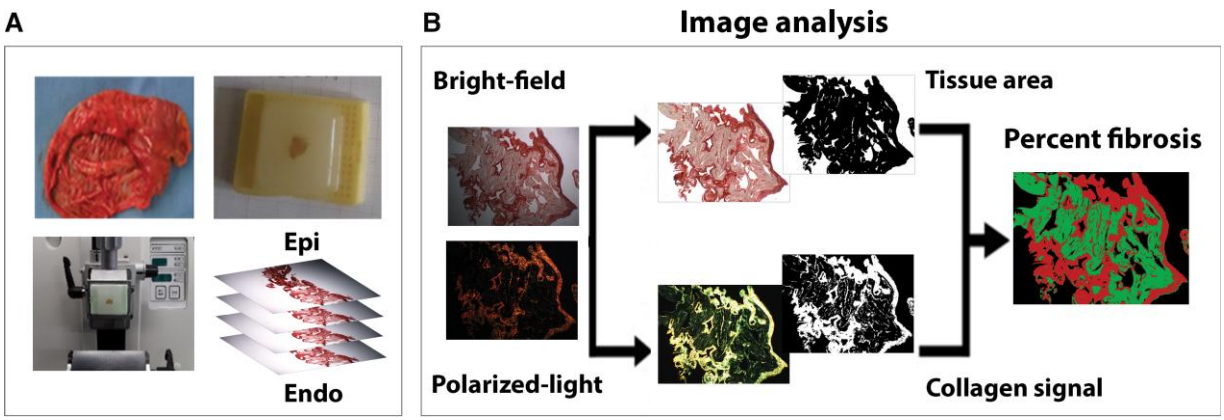

Figure 1 Slice-by-slice quantification of intramural fibrosis in human atrial tissue. (*A*) Series of 5 μm thick atrial slices obtained by microtome cutting of right atrial appendage tissue. Cuts were performed tangentially to the epicardial/endocardial surface. (*B*) Transmural fibrosis quantification by picrosirius red staining and computerized image analysis. Stained sections were examined in bright-field (top) and polarized light microscopy (bottom). A custom-made image software quantified fibrosis fraction [ratio of collagen area (red) to segmented tissue area (green), in percentage] at 5 μm slice resolution. See text for details.

Statistical analysis

Categorical variables were expressed as numbers or percentages. Continuous variables were expressed as mean ± standard deviation or median (interquartile range) according to data normality (Shapiro–Wilk test). Statistical differences among patient subgroups were consistently evaluated by one-way analysis of variance (ANOVA) or Kruskal–Wallis test, followed by *post-hoc* multiple comparison tests with Bonferroni correction. A *P*-value <0.05 was considered statistically significant.

The relationship between 3D collagen profile parameters and atrial dilatation grade was assessed by Spearman's correlation coefficient (ρ). All the analyses were performed in Matlab R2019a (The MathWorks, Inc., Natick, MA, USA).

Results

Decreasing profile of intramural fibrosis pointed out by slice-to-slice histology

Figure 2A displays a representative example of the transmural fibrosis profile in the human atrium, obtained by the semi-automatic quantification of fibrosis applied to 5 μm serial tissue sections encompassing the entire atrial wall thickness. The fibrotic content showed a decreasing profile along tissue depth from the epicardium to the endocardium. Consistently, the polarized light images taken at progressively deeper layers (*Figure 2B*) and the corresponding 3D reconstruction (see Supplementary material online, *Figure S1*) showed the gradual reduction of collagen area along tissue depth. Despite patient-specific differences in fibrotic content values, this epi-endocardial gradient of fibrosis was consistently observed in all the patients (*Figure 2C*). The average trend in *Figure 2D* showed that collagen content rapidly decreased from 68.6 ± 11.6 to 41.2. ± 15.6% within the first 20% of depth, it underwent a further reduction to 16.5 ± 9.6% at 50% of depth, and it reached a steady state of low fibrosis values (10–13%) in the midwall and subendocardial layers.

Fast and slow decay of intramural fibrosis in normal and dilated atria

The association between the transmural profile of fibrosis and the presence of atrial dilatation and/or AF was investigated by classifying the patients into three subgroups. The control group included patients with no history of AF and atria of normal dimension to mild dilatation (Grades 0–1). The atrial dilatation group included patients with no history of AF and moderate-to-severe dilatation (grades 2–3). The AF group included patients with persistent AF associated with atrial dilatation. The clinical characteristics of the three patient subgroups are reported in *Table 1*. The transmural distributions of fibrosis in representative patients with non-dilated vs. dilated atria (*Figure 3A*) showed a fast exponential decay of intramural fibrosis in the former (spatial decay constant: 55 μm) and a slower and delayed decay in the latter (250 μm, *Figure 3A*). Consistently, the polarized light images (*Figure 3B*) and the 3D reconstruction of fibrosis (see Supplementary material online, *Figure S1*) showed that collagen areas in deeper layers were larger in dilated than normal atria. These two distinct profiles of fibrosis were reproducible within the two subgroups of sinus rhythm patients (*Figure 3C* and 3D), and were corroborated by exponential fitting (see Supplementary material online, *Table S3*). In control patients, the average level of fibrosis rapidly decreased to 11.7 ± 4.2% within 40% of tissue depth (*Figure 3E*) and the exponential fit showed short spatial decay constants (80.9 ± 24.4 μm), while in atrial dilatation patients, fibrosis slowly decreased to 31.9 ± 17.1% at 40% of depth and it stabilized around 10% only at depth ratios >70%, resulting in significantly longer decay constants (171.2 ± 54.5 μm, $P < 0.005$). Consistently, the amount of fibrosis in the midwall layers was higher in atrial dilatation patients (25 ± 13.7%) than in controls (10 ± 3.0%, $P < 0.05$), while no significant difference was observed in deeper layers. The exponential profile in the control group was highly reproducible among patients, while more irregular profiles were observed in atrial dilatation patients (goodness of fit, rmse: 3.93 vs. 5.23).

Transmural fibrotic profile in fibrillating atria

Atrial fibrillation patients showed a decreasing although highly variable transmural fibrotic profile (*Figure 4A–D*). A slow spatial decay of intramural fibrosis was observed in all AF patients (*Figure 4C*), concurrent with the slow fading of the collagen signal (*Figure 4B* and see Supplementary material online, *Figure S1*). Four over eight patients showed a sigmoidal profile (representative example in *Figure 4A*), characterized by a plateau of high fibrotic content in the subepicardial region and a subsequent slow decay to stable low fibrosis levels. A biatrial

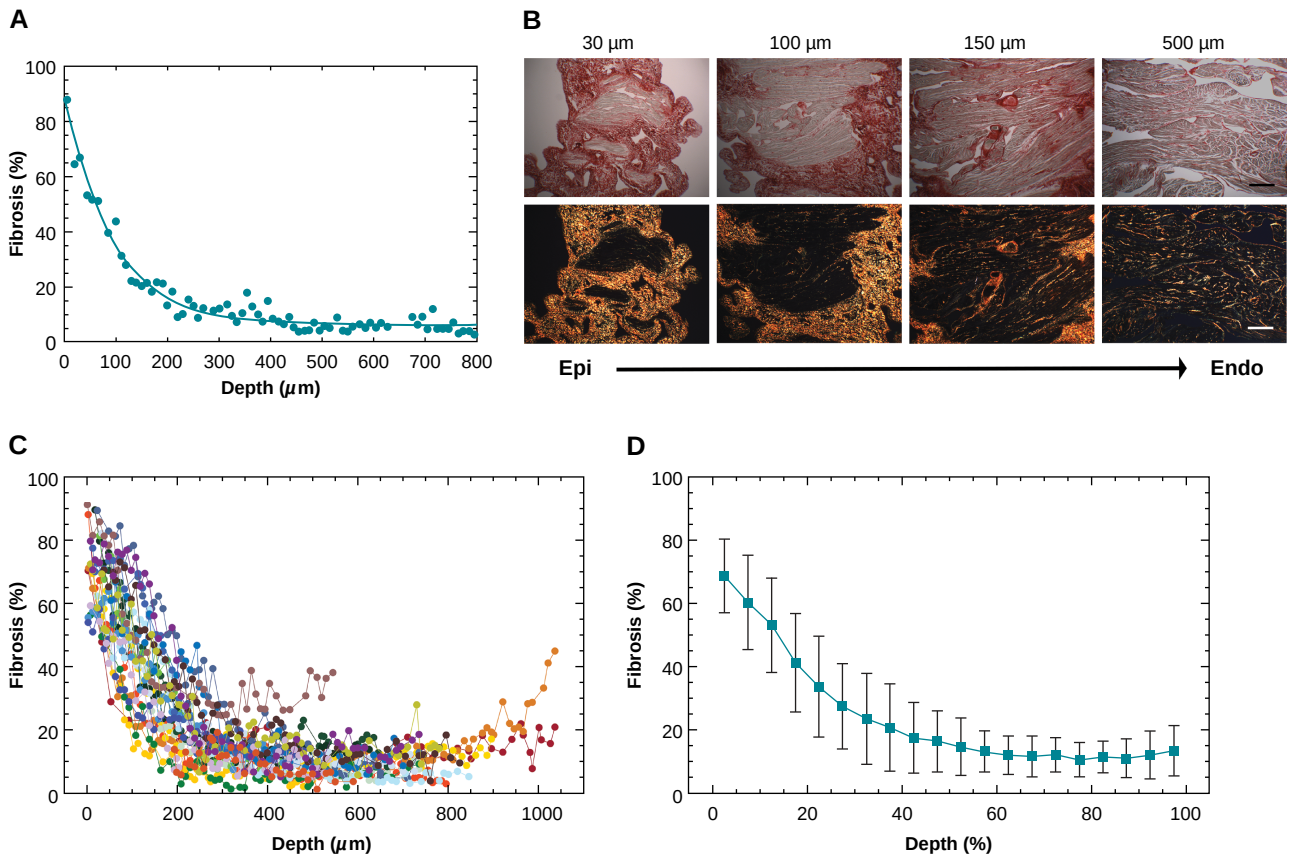

Figure 2 Transmural fibrosis profile in human atrial tissue. (*A*) Fibrosis fraction as a function of the distance from the epicardium in a representative patient. (*B*) Bright-field (top) and polarized light (bottom) images of tissue slices at increasing distance from the epicardium. Scale bar: 200 μm. (*C*) Transmural fibrosis profiles in the overall population ($n = 23$). Different colours and symbols indicate distinct patients. (*D*) Average transmural fibrosis profile over the population. To align patients' profiles, distance was expressed in relative units (ratio, %).

sigmoidal profile of fibrosis was observed in a patient with AF, where samples from both atria were available (see Supplementary material online, *Figure S2*). As shown by the average fibrosis profile of the AF group (*Figure 4D*), the amount of fibrosis was 63.3 ± 7.2% within 15% of tissue depth, it slowly decreased to 17.9 ± 6.2% in the midwall region, and it remained stable around 14.0 ± 1.2% in the subendocardial–endocardial region. The average decay constant in AF patients was 142.8 ± 41.7 μm.

Figure 5 summarizes the spatial decay constants and intramural fibrosis content within the subepicardial layers, midwall region, and subendocardial layers in the three subgroups of patients. The overall amount of fibrosis was significantly higher in atrial dilatation (29.6 ± 9.9%, $P < 0.01$) and AF (27.5 ± 7.1%, $P < 0.05$) patients compared with controls (17.0 ± 3.9%). The decay constant and the amounts of subepicardial and midwall fibrosis were significantly higher in atrial dilatation and AF patients than in controls ($P < 0.01$), while no statistically significant difference was observed between atrial dilatation and AF patients (*Figure 5*). In contrast, the extent of fibrosis in the subendocadial layers was comparable in the three patient subgroups.

Relationship between transmural fibrotic profile and atrial dilatation

To assess the relationship between atrial dilatation and transmural fibrosis, the spatial decay constant and the penetration of fibrosis were analysed as a function of atrial dilatation grade in the overall population of patients (*Figure 6*). A strong positive correlation was found between atrial dilatation grade and both the decay constant ($\rho = 0.67$, $P < 0.001$) and the intramural penetration of fibrosis ($\rho = 0.75$, $P < 0.0001$). When focusing on different transversal regions (see Supplementary material online, *Figure S3*), the extent of fibrosis strongly correlated with the atrial dilatation grade in the subepicardial ($\rho = 0.73$, $P < 0.0001$) and midwall layers ($\rho = 0.72$, $P < 0.001$), while correlation was lost for the subendocardial layers ($\rho = 0.18$, $P =$ NS).

Discussion

In this study, we reconstructed for the first time the transmural profile of atrial fibrosis in humans by a high-resolution analysis of serial microtome-cut atrial tissue slices. The study pointed out that: (i) fibrosis displayed a progressive decrease from the epicardial to the endocardial layers in all patients; (ii) a fast epi-endocardial decay was observed in sinus rhythm patients with normal atrial size; (iii) a slower decay and higher penetration of fibrosis in the subepicardial and midwall layers was observed in atrial dilatation and AF patients; and (iv) the spatial decay constant and the penetration of fibrosis in subepicardial and midwall layers correlated with the atrial dilatation grade.

In this study, we applied a novel 3D histology framework, which combined sample sequential longitudinal cutting and staining with polarized light microscopy and computer-aided image analysis. The

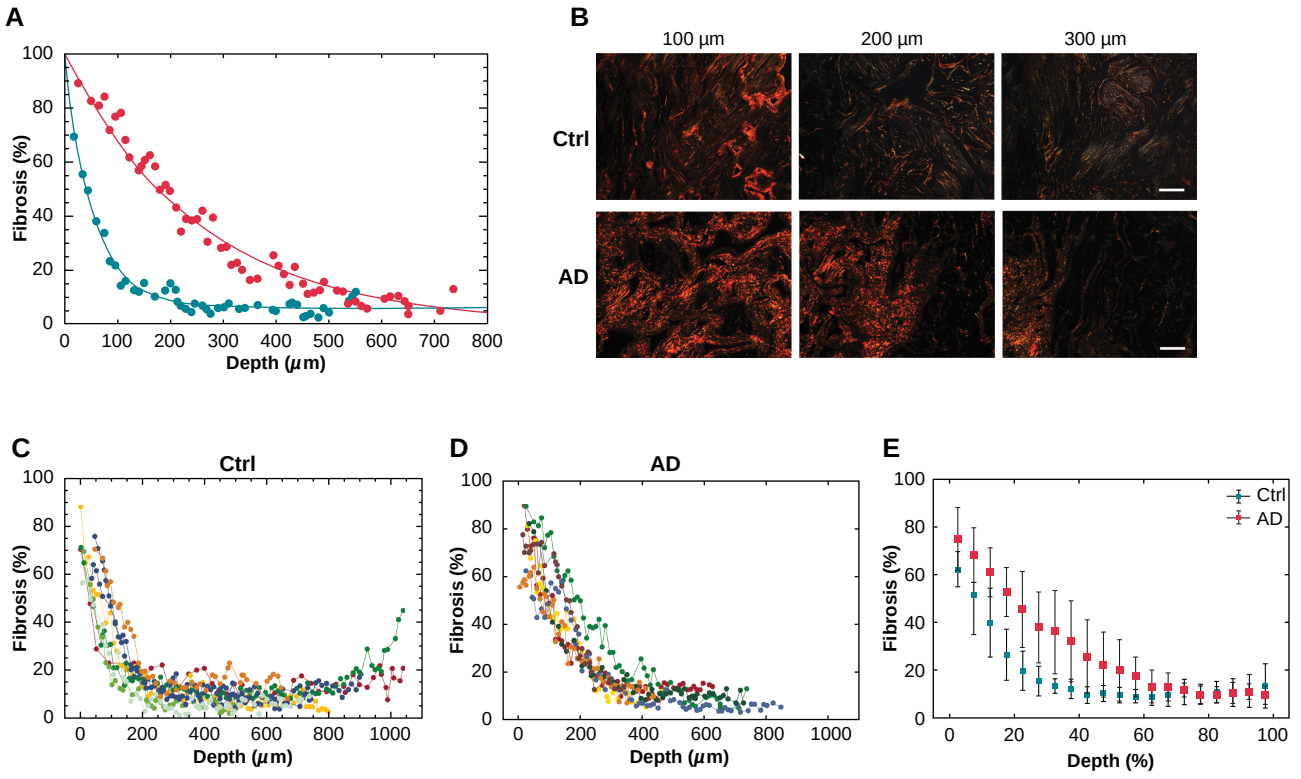

Figure 3 Transmural fibrosis profiles in sinus rhythm patients with normal atrial size (Ctrl) vs. dilated atria (AD). (*A*) Fibrosis fraction as a function of the distance from the epicardium in two representative patients with non-dilated (blue dots) and dilated atria (red dots), respectively. Exponential fits are superimposed to experimental data points. (*B*) Polarized light images of tissue slices at increasing distance from the epicardium in the patients with normal (top) and dilated atria (bottom). Scale bar: 100 μm. Transmural fibrosis profiles in the groups of patients with normal atrial size (*C*, $n = 8$) and dilated atria (*D*, $n = 7$). Different colours and symbols indicate distinct patients. (*E*) Average transmural fibrosis profile for the two patient subgroups. To align patients' profiles, distance was expressed in relative units (ratio, %).

procedure allowed us to reconstruct with high resolution the 3D organization of transmural fibrosis in cardiac surgery patients characterized by distinct atrial dilatation grades and arrhythmic profiles. In particular, the use of serial microtome-cut longitudinal slices, sampling the whole atrial wall at a resolution of 5 μm, granted wide-view images in the longitudinal plane and high resolution along the atrial wall depth. Most previous studies provided instead a global quantification of fibrosis in the human atrial tissue by analysing cross-sections (i.e. transversally cut samples with narrow view) of atrial biopsies in different classes of patients.[11,12] Fibrotic content showed some degree of variability among studies, ranging between 5 and 16% in patients without AF[11,12] and between 22 and 28% in patients with AF.[12] Consistently with these works, we found a global content of fibrosis over the whole atrial thickness of 17 and 27.5% in the control and AF groups, respectively.

Beyond the overall quantification of fibrosis, our study provided for the first time the quantitative description of fibrosis transmural profile. All the patients displayed a progressive decrease of fibrosis from the outer epicardial layer to the trabeculated endocardial network, although AF patients showed significantly higher amounts of fibrosis in the subepicardial/midwall layers. Our results are consistent with and complement most of the studies that provided data on intramural fibrosis distribution.[7,15,16,17] Higher levels of fibrosis in the thin epicardial layer than in the endocardial network were observed in goat models of short- and long-term AF.[15] The amount of endomysial fibrosis was significantly larger in the long-term group, especially in the epicardial layer.[15] In a sterile pericarditis canine model, the volume of atrial fibroblasts was shown to decrease from the epicardial to the endocardial layer, concurrently with the increase of atrial myocyte volume.[16] In atrial samples from cardiac surgery patients, subepicardial fatty infiltrations were commonly encountered in most patients, but fibro-fatty infiltrations predominated in patients with permanent AF.[7] Interestingly, in samples with the highest amount of visually assessed fibrotic remodelling, the epicardial region clearly demonstrated a higher percentage of fibrosis and less adipose tissue, suggesting the existence of an inverse/direct relationship between adipose tissue/fibrosis and the extent of remodelled epicardium.[7]

Our results complement these findings showing that a remodelled 3D profile, similar to that of AF patients, is present also in patients with atrial dilatation. The relationship between structural remodelling and atrial overload was corroborated by the significant positive correlation observed between atrial fibrosis content and atrial dilatation grade in the whole study population. Although a correlation between the global amount of fibrosis and atrial dilatation was previously pointed out,[12] we showed that this relationship mainly owed to subepicardial/midwall fibrosis, while no correlation between atrial dilatation grade and subendocardial fibrosis was observed. This may suggest a specific action of atrial overload on fibrosis development in the external atrial layers. The higher degree of fibrosis in the epicardial/subepicardial layers of atrial dilatation/AF patients may be explained in the light of the emerging properties of this region.[17] The thin epicardial layer

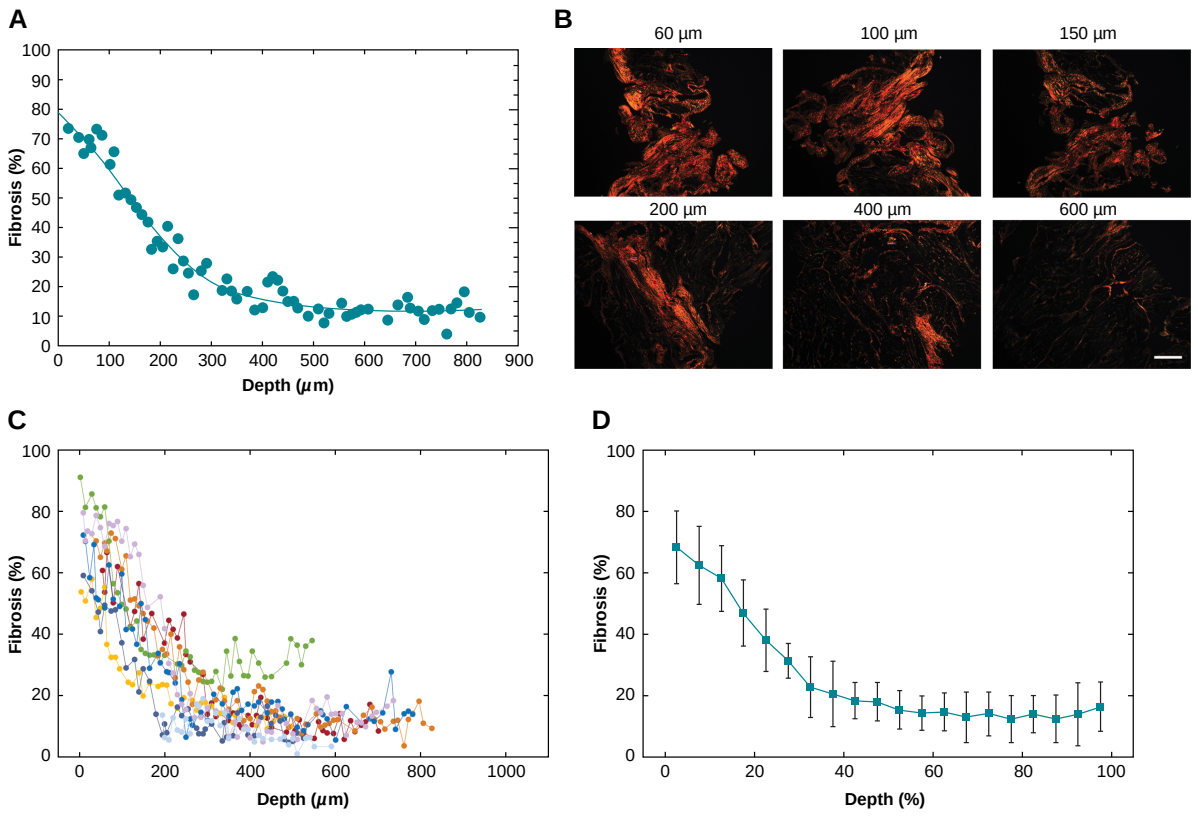

Figure 4 Transmural fibrosis profile in atrial fibrillation (AF) patients. (*A*) Fibrosis fraction as a function of the distance from the epicardium in a representative AF patient. (*B*) Polarized light images of tissue slices at increasing distance from the epicardium. Scale bar: 500 μm. (*C*) Transmural fibrosis profile in the AF patient group ($n = 8$). Different colours and symbols indicate distinct patients. (*D*) Average transmural fibrosis profile in the AF group. To align patients' profiles, distance was expressed in relative units (ratio, %).

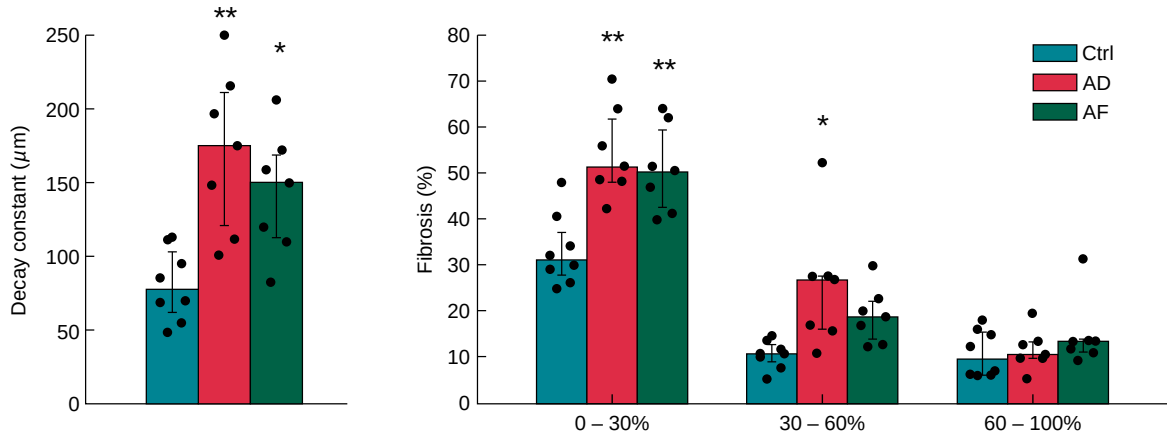

Figure 5 Characteristics of transmural fibrosis in control (ctrl, $n = 8$), atrial dilatation (AD, $n = 7$), and atrial fibrillation (AF, $n = 7$; one patient was excluded due to the incomplete fibrosis profile) patients. Fibrosis spatial decay constant (right) and fibrosis content (left) in subepicardial (0–30% depth), midwall (30–60% depth), and subendocardial layers (60–100% depth) in the three patient subgroups. *$P < 0.05$ vs. control. **$P < 0.01$ vs. control). Bars indicate median values and whiskers interquartile values.

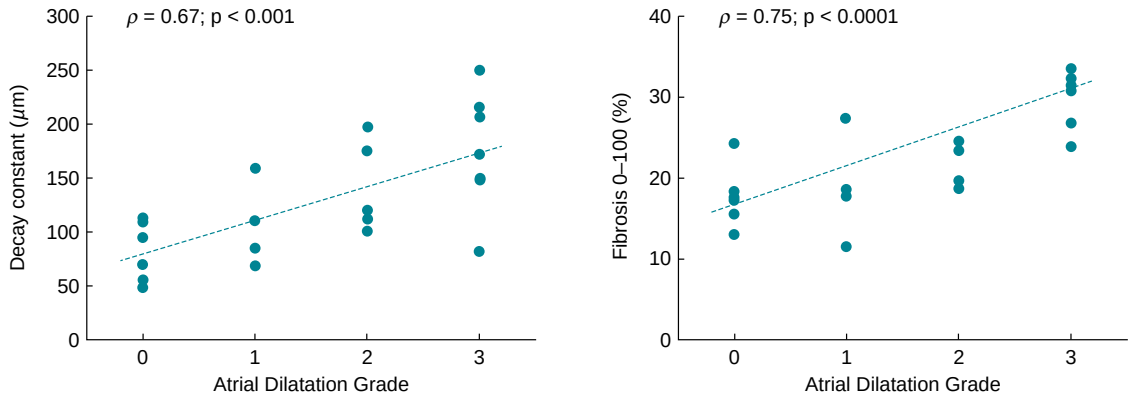

Figure 6 Relationship between intramural fibrosis penetration and atrial dilatation (AD). Spatial decay constant (left) and overall content (right) of fibrosis as a function of AD grade in the patient population ($n = 22$; one atrial fibrillation patient was excluded due to the incomplete fibrosis profile). Regression lines are indicated as dotted lines. ρ, Spearman's correlation coefficient.

may experience a larger degree of stretch than the underlying network of trabeculae, which may translate into a larger stimulus for fibrosis formation.[15] Through the mediation of Angiotensin II and atrial natriuretic peptide, atrial stretch may in turn stimulate the reactivation and differentiation into myofibroblasts of progenitor cells present in the epicardium, which may promote the fibrotic remodelling of neighbouring layers.[17]

The observed spreading of fibrosis from the epicardial layer to the neighbouring subepicardial myocardium may concur to disrupt the electrical continuity of the atrial myocardial tissue, contributing to the formation of a 3D substrate and potentially to AF promotion.[9,15] The proarrhythmic role of intramural fibrosis in human hearts is testified by accumulating evidence from experimental,[5,8] clinical,[10,18,19,20] and simulation studies.[4,21] Mapping studies in cardiac surgery patients showed higher incidence of epicardial breakthroughs in long-standing persistent forms of AF[19] and a correlation between AF complexity and the amount of endomysial fibrosis.[20] These results may suggest that conduction disturbances within the epicardial layer could be ascribed to the duration of AF and the higher complexity of the 3D substrate in chronically dilated atria. Consistently, in realistic AF models, a complex intramural microstructure of fibrosis supported stable re-entries,[4] and a higher amount of epicardial fibrosis could explain an increased epi-endocardial dissociation and an augmented incidence of breakthroughs.[21]

Study limitations

This study has several limitations. First, it is characterized by a small population of valvular disease patients, which partially limits extrapolation of our findings to wider populations and precluded the evaluation of the effects of additional factors and/or comorbidities on fibrosis occurrence and pattern. Moreover, due to the characteristics of the study population, the control group included patients with pathologies, which may affect atrial function and structure.

Second, due to the restrictions imposed by the cardiac surgery setting, only small right atrial appendage specimens were systematically analysed in the study population. Therefore, the observed transmural profile cannot be generalized to other right atrial areas nor to left atrial regions that play a major role in AF.

Although different types of fibrosis may have different implications on arrhythmias,[6,20] we provided only a global quantification of fibrosis without subclassification of fibrosis quality. Moreover, no electrocardiographic data were acquired in the study population.

Finally, due to the observational nature of our study and the limitations of correlation analysis, we could only show an association between atrial dilatation, rhythm, and fibrosis transmural profiles. Further studies are thus needed to directly prove cause–effect relationships between atrial stretch, AF, and fibrosis burden.

Conclusion

In this study, we showed for the first time the transmural profile of fibrosis in the human atrium at high spatial resolution. The profile was characterized by a decreasing content of fibrosis from the epicardium to the endocardium. We showed a deeper penetration of fibrosis in the atrial wall of AF patients, which was closely related to the degree of atrial dilatation. This experimental evidence constitutes a first step towards a complete understanding of the deleterious interaction between atrial fibrosis and atrial dilatation in the maintenance of AF.

Supplementary material

Supplementary material is available at *Europace* online.

Funding

This work was supported by Fondazione Cassa di Risparmio di Trento e Rovereto (grant no. 2011.0194 to F.R.).

Conflict of interest: None declared.

Data availability

The data underlying this article will be shared on reasonable request to the corresponding author.

References

1. Nattel S. Molecular and cellular mechanisms of atrial fibrosis in atrial fibrillation. *JACC Clin Electrophysiol* 2017;**3**:425–35.
2. Carver W, Goldsmith EC. Regulation of tissue fibrosis by the biomechanical environment. *Biomed Res Int* 2013;**2013**:101979.
3. Disertori M, Masè M, Ravelli F. Myocardial fibrosis predicts ventricular tachyarrhythmias. *Trends Cardiovasc Med* 2017;**27**:363–72.

4. Chen R, Wen C, Fu R, Li J, Wu J. The effect of complex intramural microstructure caused by structural remodeling on the stability of atrial fibrillation: insights from a three-dimensional multi-layer modeling study. *PLoS One* 2018;**13**:e0208029.
5. Hansen BJ, Zhao J, Csepe TA, Moore BT, Li N, Jayne LA *et al.* Atrial fibrillation driven by micro-anatomic intramural re-entry revealed by simultaneous sub-epicardial and sub-endocardial optical mapping in explanted human hearts. *Eur Heart J* 2015;**36**:2390–401.
6. Verheule S, Schotten U. Electrophysiological consequences of cardiac fibrosis. *Cells* 2022;**10**:3220.
7. Haemers P, Hamdi H, Guedj K, Suffee N, Farahmand P, Popovic N *et al.* Atrial fibrillation is associated with the fibrotic remodelling of adipose tissue in the subepicardium of human and sheep atria. *Eur Heart J* 2017;**38**:53–61.
8. Zhao J, Hansen BJ, Wang Y, Csepe TA, Sul LV, Tang A *et al.* Three-dimensional integrated functional, structural, and computational mapping to define the structural "fingerprints" of heart-specific atrial fibrillation drivers in human heart ex vivo. *J Am Heart Assoc* 2017;**6**:e005922.
9. Eckstein J, Zeemering S, Linz D, Maesen B, Verheule S, van Hunnik A *et al.* Transmural conduction is the predominant mechanism of breakthrough during atrial fibrillation: evidence from simultaneous endo-epicardial high-density activation mapping. *Circ Arrhythm Electrophysiol* 2013;**6**:334–41.
10. de Groot N, van der Does L, Yaksh A, Lanters E, Teuwen C, Knops P *et al.* Direct proof of endo-epicardial asynchrony of the atrial wall during atrial fibrillation in humans. *Circ Arrhythm Electrophysiol* 2016;**9**:e003648.
11. Goette A, Juenemann G, Peters B, Klein HU, Roessner A, Huth C *et al.* Determinants and consequences of atrial fibrosis in patients undergoing open heart surgery. *Cardiovasc Res* 2002;**54**:390–6.
12. Platonov PG, Mitrofanova LB, Orshanskaya V, Ho SY. Structural abnormalities in atrial walls are associated with presence and persistency of atrial fibrillation but not with age. *J Am Coll Cardiol* 2011;**58**:2225–32.
13. Lang RM, Bierig M, Devereux RB, Flachskampf FA, Foster E, Pellikka PA *et al.* Recommendations for chamber quantification. *Eur J Echocardiogr* 2006;**7**:79–108.
14. Hadi AW, Mouchaers KTB, Schalij I, Grunberg K, Meijer GA, Vonk-Noordegraaf A *et al.* Rapid quantification of myocardial fibrosis: a new macro-based automated analysis. *Cell Oncol* 2011;**34**:343–54.
15. Verheule S, Tuyls E, Gharaviri A, Hulsmans S, van Hunnik A, Kuiper M *et al.* Loss of continuity in the thin epicardial layer because of endomysial fibrosis increases the complexity of atrial fibrillatory conduction. *Circ Arrhythm Electrophysiol* 2013;**6**:202–11.
16. Ryu K, Li L, Khrestian CM, Matsumoto N, Sahadevan J, Ruehr ML *et al.* Effects of sterile pericarditis on connexins 40 and 43 in the atria: correlation with abnormal conduction and atrial arrhythmias. *Am J Physiol Heart Circ Physiol* 2007:**293**:H1231–41.
17. Suffee N, Moore-Morris T, Jagla B, Mougenot N, Dilanian G, Berthet M *et al.* Reactivation of the epicardium at the origin of myocardial fibro-fatty infiltration during the atrial cardiomyopathy. *Circ Res* 2020;**126**:1330–42.
18. Goette A, Kalman JM, Aguinaga L, Akar J, Cabrera JA, Chen SA *et al.* EHRA/HRS/APHRS/SOLAECE expert consensus on atrial cardiomyopathies: definition, characterisation, and clinical implication. *J Arrhythm* 2016;**32**:247–78
19. de Groot NM, Houben RP, Smeets JL, Boersma E, Schotten U, Schalij MJ *et al.* Electropathological substrate of longstanding persistent atrial fibrillation in patients with structural heart disease: epicardial breakthrough. *Circulation* 2010;**122**:1674–82.
20. Maesen B, Verheule S, Zeemering S, La Meir M, Nijs J, Lumeij S *et al.* Endomysial fibrosis, rather than overall connective tissue content, is the main determinant of conduction disturbances in human atrial fibrillation. *Europace* 2022;**24**:1015–24.
21. Gharaviri A, Bidar E, Potse M, Zeemering S, Verheule S, Pezzuto S *et al.* Epicardial fibrosis explains increased endo-epicardial dissociation and epicardial breakthroughs in human atrial fibrillation. *Front Physiol* 2020;**11**:68.